Author Manuscript

Author Manuscript

Author Manuscript

Author Manuscript

HHS Public Access

Author manuscript

AJR Am J Roentgenol. Author manuscript; available in PMC 2018 March 01.

Published in final edited form as:

AJR Am J Roentgenol. 2017 March ; 208(3): W85–W91. doi:10.2214/AJR.16.16652.

Differentiation of Clear Cell Renal Cell Carcinoma From Other Renal Cortical Tumors by Use of a Quantitative Multiparametric MRI Approach

Andreas M. Hötker[1,2], **Yousef Mazaheri**[3], **Andreas Wibmer**[1], **Christoph A. Karlo**[1], **Junting Zheng**[4], **Chaya S. Moskowitz**[4], **Satish K. Tickoo**[5], **Paul Russo**[6], **Hedvig Hricak**[1], and **Oguz Akin**[1]

[1]Department of Radiology, Memorial Sloan-Kettering Cancer Center, 1275 York Ave, New York, NY 10065

[2]Department of Diagnostic and Interventional Radiology, Universitätsmedizin Mainz, Mainz, Germany

[3]Department of Medical Physics, Memorial Sloan-Kettering Cancer Center, New York, NY

[4]Department of Epidemiology and Biostatistics, Memorial Sloan-Kettering Cancer Center, New York, NY

[5]Department of Pathology, Memorial Sloan-Kettering Cancer Center, New York, NY

[6]Department of Surgery, Urology Service, Memorial Sloan-Kettering Cancer Center, New York, NY

Abstract

OBJECTIVE—The purpose of this study was to develop a quantitative multiparametric MRI approach to differentiating clear cell renal cell carcinoma (RCC) from other renal cortical tumors.

MATERIALS AND METHODS—This retrospective study included 119 patients with 124 histopathologically confirmed renal cortical tumors who underwent preoperative MRI including DWI, contrast-enhanced, and chemical-shift sequences before nephrectomy. Two radiologists independently assessed each tumor volumetrically, and apparent diffusion coefficient values, parameters from multiphasic contrast-enhanced MRI (peak enhancement, upslope, downslope, AUC), and chemical-shift indexes were calculated. Univariate and multivariable logistic regression analyses were performed to identify parameters associated with clear cell RCC.

RESULTS—Interreader agreement was excellent (intraclass correlation coefficient, 0.815–0.994). The parameters apparent diffusion coefficient (reader 1 AUC, 0.804; reader 2, 0.807), peak enhancement (reader 1 AUC, 0.629; reader 2, 0.606), and downslope (reader 1 AUC, 0.575; reader

Address correspondence to A. M. Hötker (Andreas.Hoetker@uni-mainz.de).

This study expands on our earlier investigation (*AJR* 2016; 206:100–105), in which only DWI results were analyzed. For the current study, similar measurements were added for contrast-enhanced and chemical-shift MRI sequences, which were part of the dedicated renal MRI protocol for all patients.

Based on a presentation at the European Congress of Radiology 2015 annual meeting, Vienna, Austria (abstract published in *Insights Imaging* 2015; 6(suppl 1):S380).

Author Manuscript Author Manuscript Author Manuscript Author Manuscript

2, 0.561) were significantly associated with discriminating clear cell RCC from other renal cortical tumors. The combination of all three parameters further increased diagnostic accuracy (reader 1 AUC, 0.889; reader 2, 0.907; both $p \leq 0.001$), yielding sensitivities of 0.897 for reader 1 and 0.897 for reader 2, and specificities of 0.762 for reader 1 and 0.738 for reader 2 in the identification of clear cell RCC. With maximized sensitivity, specificities of 0.429 and 0.262 were reached for readers 1 and 2, respectively.

CONCLUSION—A quantitative multiparametric approach statistically significantly improves diagnostic performance in differentiating clear cell RCC from other renal cortical tumors.

Keywords

diagnostic imaging; diffusion; DWI; kidney; MRI; neoplasms; renal cell carcinoma

---

It is estimated [1] that in 2016, more than 60,000 people in the United States had a new diagnosis of kidney cancer (including tumors originating from the renal pelvis). Of the various subtypes of renal cell carcinoma (RCC), clear cell RCC is the most common and aggressive. It accounts for most cases of metastasis and is associated with worse outcomes than, for example, papillary and chromophobe RCC [2]. However, given that many renal tumors are incidentally found in frail and elderly patients and that 10–30% of re-sected tumors prove to be benign at histopathologic analysis [3], options such as active surveillance and focal ablation have been introduced to patient care. These alternatives are considered for selected patients for whom less invasive treatment is preferred to radical or partial nephrectomy (the current standard of care). The introduction of these less invasive alternatives has created a great clinical need to correctly characterize renal lesions before treatment selection to avoid undertreatment. Because the role of renal biopsy is still evolving, studies are focusing on approaches to noninvasively identifying aggressive subtypes of RCC by use of imaging.

Clear cell RCC is known to be a highly vascular tumor compared with, for example, papillary RCC. Therefore, some studies [4– 6] have examined whether the contrast enhancement of a renal tumor at CT or MRI can be used to differentiate clear cell RCC from less aggressive subtypes and from benign tumors. Some investigators [7, 8] have attempted to characterize renal tumors on the basis of the apparent diffusion coefficient (ADC), a measure of cell density derived from DWI. Others have attempted to use chemical-shift MRI to quantify intracellular fat content (a feature thought to be predominantly present in clear cell RCC and angiomyolipoma) [6, 9] or investigated differences in FDG uptake between tumor subtypes [10]. These approaches have provided valuable insights into the imaging characteristics of RCC subtypes. However, they share a common problem that limits their diagnostic value: for each metric applied, the ranges of values found in different renal cortical tumors overlap greatly. The purpose of this study was to develop a dedicated quantitative multiparametric MRI approach to correct pretreatment characterization of newly discovered renal cortical lesions.

Author Manuscript Author Manuscript Author Manuscript Author Manuscript

Materials and Methods

Patients and Inclusion Criteria

This HIPAA-compliant study received institutional review board approval, and the requirement for informed consent was waived. We retrospectively searched the urology, radiology, and pathology databases at one institution for the time interval March 2006 to April 2013 to identify patients who had newly diagnosed renal cortical tumors and underwent MRI examinations with a dedicated renal MRI protocol before undergoing total or partial nephrectomy at that institution. We identified 119 patients with 124 renal cortical tumors fulfilling the inclusion criteria. Among the 119 patients, two were exempt from analysis of DW images owing to heavy distortion. Two other patients were excluded from analysis of contrast-enhanced MR images: one because of failure of fat saturation and another because of motion artifacts. The mean interval between MRI examination and surgery was 37 days (range, 1–250 days).

MRI Technique and Analysis and Standard of Reference

MRI examinations were performed with a dedicated renal MRI protocol at a field strength of 1.5 T. The protocol included a DWI sequence with b values of 0 and 500 s/mm^2 (echo-planar imaging sequence; breath-hold; TR/TE, 1800–6000/59.2– 84.3; matrix, 96 × 96 to 128 × 128; FOV, 440–460 mm; slice thickness, 7-mm; intersection gap, 1 mm), T1-weighted fat-saturated multiphase contrast-enhanced imaging (TR/TE, 3.48–6.64/1.64–3.26; flip angle, 12°; matrix, 256 × 160–192; FOV, 320–400 mm; slice thickness, 5 mm; intersection gap 2.5 mm), and a chemical-shift sequence (TR/TE, 215– 275/2.2 and 4.4; matrix, 256 × 256; FOV, 320–400 mm; slice thickness, 8-mm; no intersection gap). A voxelwise ADC map was generated using a mono-exponential model. T2-weighted sequences in axial and coronal orientations were also performed for each patient to aid tumor localization.

Two radiologists with 4 and 6 years of experience in reading MR images, both participating in a dedicated fellowship program for genitourinary MRI research, independently analyzed the MRI examinations. The readers were blinded to all histopathologic and clinical patient data. After identifying the tumor using all available sequences, each reader used ImageJ software (version 1.47 m, National Institutes of Health) [11] to place an ROI around the tumor on each slice with visible tumor. In this way they volumetrically assessed the entire tumor in each sequence (Fig. 1). Care was taken not to include any surrounding tissue in the measurements. In cystic tumors, only the solid component was evaluated. This method was performed independently on the ADC map, on each image obtained with the T1-weighted fat-saturated multiphase contrast-enhanced sequence, and on both the in-phase and the opposed-phase chemical-shift images. ROIs were drawn independently on images from the unenhanced, corticomedullary, nephrographic, and excretory phases of contrast enhancement to account for slight patient movement and differences in breathing between phases.

The data from all ROIs were analyzed with inhouse software written in the Matlab language (Version R2014b, MathWorks). First, mean ADC values were calculated for each tumor on a

Author Manuscript Author Manuscript Author Manuscript Author Manuscript

voxel-by-voxel basis. Then, analysis of contrast-enhanced image data was performed as follows.

The enhancement of a lesion at time *t* was expressed according to the following equation:

$$enhancement\,(t) = \frac{SI_{post}\,(t) - SI_{pre}\,(0)}{SI_{pre}\,(0)} \times 100, \quad (1)$$

where $SI_{pre}(0)$ is the unenhanced signal intensity and $SI_{post}(t)$ is the contrast-enhanced signal intensity at time *t*. When enhancement is plotted over time, enhancement curves can be generated.

A linear-slope model was developed to model the data, which were fitted to the following equation:

$$enhancement\,(t) = \begin{cases} US \times t & t \leq TTP \\ US \times TTP + DS\,(t - TTP) & t > TTP \end{cases}, \quad (2)$$

where *US* is upslope, *t* is time, *TTP* is time to peak enhancement, and *DS* is downslope.

The following parameters were derived from the fitted enhancement curve on a pixelwise basis: peak enhancement, upslope, downslope, and AUC at 100 seconds (integral of the AUC). Peak enhancement refers to the maximum enhancement during contrast uptake (in percentages). The contrast wash-in occurs between the start of injection and the time of peak enhancement. Upslope is the corresponding slope of the contrast wash-in. The unit is change in signal intensity per second (ΔSI/s), and downslope is the slope of the descending curve during washout and is measured between the time of the maximal enhancement and the last acquisition, also in ΔSI/s.

For chemical-shift imaging, the chemical-shift index [9] is expressed as a percentage, that is, $[(SI^{op} - SI^{in}) / SI^{in}] \times 100$, where *op* is opposed-phase and *in* is in-phase imaging. The volume of all voxels with a decrease of at least 10% in signal intensity between in-and opposed-phase imaging (chemical-shift volume drop, expressed as a percentage of whole tumor volume) were evaluated for each tumor. The threshold of 10% was applied to reduce the effect of noise on the measurements. It was chosen in light of earlier investigations that showed a mean decrease in chemical-shift index of more than 10% in clear cell RCC [9].

Surgical histopathologic analysis of the resected specimen served as the reference standard. All pathologic examinations were performed by an experienced genitourinary pathologist.

Statistical Methods

Interreader agreement on each MRI parameter was assessed with the Shrout-Fleiss fixed set intraclass correlation coefficient. Univariate and multivariable generalized linear regression analyses with a logit link function were performed to identify significant parameters associated with clear cell RCC for each reader separately. To take into account multiple

Author Manuscript Author Manuscript Author Manuscript Author Manuscript

tumors per patient, generalized estimating equation methods were used in regression analyses with a robust covariance matrix and independent correlation structure. Logarithm transformation was applied to peak enhancement, upslope, and AUC in contrast-enhanced MRI. MRI parameters found to contribute significantly to the distinction between clear cell RCC and other renal cortical tumors in univariate analysis were included in the multivariable analysis, for which backward selection was used with entry and stay significant levels of 0.05.

Odds ratio and 95% CI were estimated. The nonparametric ROC curve AUC was calculated for each parameter and for the estimated probabilities of being clear cell RCC from multivariable analysis under leave-one-out cross-validation. Two cutoff values for the combination of significant parameters were identified to maximize the Youden index and sensitivity of the ROC curve separately from a multivariable analysis for each reader. Sensitivity and specificity at the cutoff point were estimated; multiple tumors per patient were accounted for by use of the generalized estimating equation method. Comparing AUCs for multiparametric MRI from the multivariable model and each parameter separately involves testing for differences in AUCs from nested models, which has been found problematic [12, 13]. We therefore followed previously published advice [12, 14] and present only results of the Wald test from the logistic model, which tests a hypothesis equivalent to the null hypothesis that the AUCs from the different models are equal. All statistical analyses were performed with SAS (version 9.2, SAS Institute) and R (version 2.13, R Foundation) software.

Results

Patients

Of the 119 patients included in this study, 85 were men (71%; mean age, 61 years; range, 31–80 years), and 34 were women (29%; mean age, 57 years; range, 17–83 years). Of the 124 tumors analyzed in these patients, 81 (65.3%) were clear cell RCC (pT1, 22; pT2, 5; pT3, 54; NX, 14; N1, 1; N0, 66), seven (5.6%) were angiomyolipoma, 12 (9.7%) were chromophobe RCC, four (3.2%) were oncocytoma, 12 (9.7%) were papillary RCC, and eight (6.5%) were unclassified RCC. The mean tumor size across all lesions was 7.16 cm (range, 1–20.5 cm). The median tumor size in the clear cell RCC group was 8 cm (range, 1–16 cm), and the median tumor size in the non-clear cell RCC group was 4.5 cm (range, 1.2–20.5 cm).

Interreader Agreement

For all MRI parameters, medians and ranges and interreader agreement levels are shown in Table 1. Interreader agreement was excellent; intraclass correlation coefficients ranged from 0.815 (downslope) to 0.994 (AUC).

Multiparametric MRI in the Identification of Clear Cell Renal Cell Carcinoma

Univariate analysis showed that the parameters ADC from DWI (odds ratio reader 1, 1.30; reader 2, 1.29; $p < 0.001$) and peak enhancement (odds ratio reader 1, 1.77; reader 2, 1.63; $p = 0.021$ reader 1, $p = 0.032$ reader 2) and downslope (odds ratio reader 1, 3.45; reader 2,

Author Manuscript Author Manuscript Author Manuscript Author Manuscript

2.27; $p = 0.009$ reader 1, $p = 0.038$ reader 2) from contrast-enhanced MRI were significantly associated with differentiating clear cell RCC from other renal cortical tumors (Table 2). All three parameters were statistically significant in multivariable analysis ($p \leq 0.001$).

For both readers, ADC values had the best diagnostic performance (AUC reader 1, 0.804; reader 2, 0.807), followed by peak enhancement (AUC reader 1, 0.629; reader 2, 0.606) and downslope (AUC reader 1, 0.575; reader 2, 0.561) (Fig. 2). The combination of all three parameters further increased diagnostic accuracy to an AUC of 0.889 for reader 1 and 0.907 for reader 2 (Table 3). Our analyses showed that the tumor was likely to be clear cell RCC when the following was true: $[-11.011 + 3221 \times \text{ADC} + 1.11 \times \log(\text{peak enhancement}) + 3.220 \times \text{downslope}] \geq 0.245$.

With use of the combination of ADC, peak enhancement, and downslope, internal validation resulted in sensitivities of 0.897 for both readers and specificities of 0.762 and 0.738 for identification of clear cell RCC by readers 1 and 2, respectively (Table 3). When sensitivity was maximized to 0.987, specificity was 0.429 for reader 1 and 0.262 for reader 2.

Discussion

The incidence of RCC in the United States has risen over several decades [1]. Surgery (partial or radical nephrectomy) remains the standard of care for young and healthy patients with these incidentally found tumors. However, the substantial number of elderly patients with such tumors poses a clinical challenge, because rates of medical comorbidities and chances of renal impairment after surgery are generally higher among these patients [15]. Conservative treatment approaches such as active surveillance and focal ablation may be considered if the tumor is thought to be of an indolent type. However, the use of renal biopsy, an invasive method for tumor characterization, is still evolving in this context [16] and is not part of the standard workup in most clinical centers. Therefore, studies have been conducted to investigate noninvasive methods of differentiating renal cortical tumors with imaging.

Given that clear cell RCC is known for being highly vascular compared with other RCC subtypes, such as chromophobe RCC and, in particular, papillary RCC [5], several groups have attempted to differentiate renal tumor subtypes on the basis of their grade of enhancement on contrast-enhanced CT [4] and MR [5, 17, 18] images. They found statistically significant differences between enhancement levels in different RCC subtypes. However, generally broad overlap of the ranges of enhancement levels in clear cell RCC and other subtypes, particularly benign oncocytoma and angiomyolipoma, rendered difficult the discrimination of clear cell RCC based on contrast enhancement alone [5, 19, 20].

DWI, which yields information about the cell density of a lesion, has been of value in several fields of oncologic imaging and has therefore also been applied to the differentiation of RCC subtypes. Most investigators reported that ADC values of clear cell RCC were significantly higher than those of other RCC subtypes but in the same range as those of benign oncocytoma [7, 8].

Author Manuscript Author Manuscript Author Manuscript Author Manuscript

Because a large amount of intracellular fat is another imaging feature thought to be predominantly present in clear cell RCC, Karlo et al. [9] investigated the use of chemical-shift MRI sequences to assess intracellular fat in renal tumors. They reported that a decrease in signal intensity of more than 25% between in-and opposed-phase imaging may be useful for differentiating clear cell RCC from other RCC subtypes. However, a comparable decrease was also seen in angiomyolipoma, which hindered the differentiation of clear cell RCC from angiomyolipoma when the pathognomonic sign of gross fat was lacking [9, 21].

We hypothesized that a quantitative multiparametric MRI approach (including contrast-enhanced, DWI, and chemical-shift imaging) may yield greater discriminatory power in identifying clear cell RCC than any of the aforementioned, single-parameter approaches. Cornelis et al. [22] also took a multiparametric approach, analyzing T2-weighted, contrast-enhanced, DWI and chemical-shift MRI findings in 100 renal cortical tumors (57 of which were clear cell RCC) in 90 patients, but they did not volumetrically assess the tumor and relied on measuring ROIs only. They found that a combination of ADC ratios and parameters from contrast-enhanced MRI (namely, wash-in and washout indexes) could differentiate papillary RCC from other renal cortical tumors with a specificity of 100%, though the sensitivity of this combination was low at 37.5%. In the same study, the use of contrast-enhanced sequences and of a signal intensity index based on chemical-shift sequences (comparable to the chemical-shift index used in our study) yielded specificity of 94.2% in differentiating oncocytoma from clear cell RCC, but sensitivity was low at 18.7%. Although some investigators used chemical-shift MRI to differentiate oncocytoma from clear cell RCC, they reported considerable overlap between those two tumor types in chemical-shift imaging [9, 21]. In our study, chemical-shift imaging was of little value. The discrepancies in the aforementioned findings may be due to differences in the patient cohorts studied, especially the varying proportions of patients with tumors of high or low Fuhrman grades, because clear cell RCCs with higher nuclear grades contain less intracellular fat than those of lower grades [23].

Our study built on the aforementioned preliminary findings by examining a larger cohort of patients and by conducting volumetric tumor assessment instead of single ROI-based analysis. We assumed that volumetric assessment may be preferable in light of the great intratumor heterogeneity of RCC [24]. Furthermore, we focused on the clinically important need to single out clear cell RCC—the most aggressive subtype—from all other subtypes, rather than comparing individual pairs of tumor subtypes.

In our study, clear cell RCC had significantly higher ADC values, higher peak enhancement, and higher washout rates (downslope) than other renal cortical tumors. These findings align well with those of previous studies [5, 7]. However, as in previous studies, the values of individual parameters overlapped between histopathologic tumor types. Though contrast-enhanced MRI is known to be helpful in differentiating RCC subtypes [5, 18], the fact that some benign tumors (i.e., oncocytoma and angiomyolipoma) are also strongly hypervascularized lessens the value of this modality when these tumors are included in the analysis [5, 19, 20].

Author Manuscript Author Manuscript Author Manuscript Author Manuscript

With sensitivity and specificity of approximately 0.900 and 0.730–0.760, the combination of ADC, peak enhancement, and downslope in our study showed considerable promise as a means of addressing the clinical need for noninvasive pretreatment characterization of renal cortical lesions. When maximizing sensitivity in the characterization of clear cell RCC, as would be necessary in the clinical setting to avoid missing an aggressive tumor, our two readers achieved specificity of 0.429 and 0.262. Additional studies would be helpful to determine whether specificity can be increased by adding innovative DWI approaches with higher b values or by performing other emerging functional MRI techniques, such as arterial spin labeling [25].

Our study had a number of limitations. Because of its retrospective nature and our requirement for histopathologic examination of resected specimens, we included only patients who underwent surgery. Though this enabled us to have a high level of confidence regarding the exact histopathologic types of the tumors assessed, in comparison with patient selection based on biopsy or follow-up examinations, it may have caused our sample to include a disproportionate number of benign tumors with atypical appearances (e.g., lipid-poor angiomyolipomas with no evidence of macroscopic fat), because patients with benign tumors of more normal appearance might have been less likely to undergo surgery. Our cohort also might have been slightly skewed toward more aggressive tumors because, for example, we did not include patients undergoing active surveillance for an undetermined kidney lesion. In addition, the exact composition of the group of tumors that were not of the clear cell RCC subtype might have influenced our results. For example, because papillary RCC is known to have both lower ADC values and is less enhancing than clear cell RCC, the presence of a large number of them might have resulted in better discrimination of clear cell RCC than would the presence of a large number of oncocytomas, which have characteristics very similar to those of clear cell RCC at both contrast-enhanced MRI and DWI [5].

Conclusion

Our study showed that compared with the use of any single MRI parameter, the use of a quantitative multiparametric MRI approach combining DWI and contrast-enhanced imaging improves the discrimination of clear cell RCC from less aggressive tumor subtypes and may play an important role in risk stratification and treatment selection in the care of patients with renal cortical tumors.

Acknowledgments

We thank Ada Muellner for editing the manuscript.

Supported by Swiss National Science Foundation grant PASMP3_134368 (C. A. Karlo) and MSKCC Biostatistics Core grant NIH P30 CA008748 (C. S. Moskowitz, J. Zheng).

References

1. American Cancer Society. Cancer facts & figures 2016. Atlanta, GA: American Cancer Society; 2016.

Author Manuscript Author Manuscript Author Manuscript Author Manuscript

2. Leibovich BC, Lohse CM, Crispen PL, et al. Histological subtype is an independent predictor of outcome for patients with renal cell carcinoma. J Urol. 2010; 183:1309–1315. [PubMed: 20171681]
3. Corcoran AT, Russo P, Lowrance WT, et al. A review of contemporary data on surgically resected renal masses: benign or malignant? Urology. 2013; 81:707–713. [PubMed: 23453080]
4. Young JR, Margolis D, Sauk S, Pantuck AJ, Sayre J, Raman SS. Clear cell renal cell carcinoma: discrimination from other renal cell carcinoma subtypes and oncocytoma at multiphasic multidetector CT. Radiology. 2013; 267:444–453. [PubMed: 23382290]
5. Vargas HA, Chaim J, Lefkowitz RA, et al. Renal cortical tumors: use of multiphasic contrast-enhanced MR imaging to differentiate benign and malignant histologic subtypes. Radiology. 2012; 264:779–788. [PubMed: 22829683]
6. Schieda N, Dilauro M, Moosavi B, et al. MRI evaluation of small (<4cm) solid renal masses: multivariate modeling improves diagnostic accuracy for angiomyolipoma without visible fat compared to univariate analysis. Eur Radiol. 2016; 26:2242–2251. [PubMed: 26486936]
7. Wang H, Cheng L, Zhang X, et al. Renal cell carcinoma: diffusion-weighted MR imaging for subtype differentiation at 3.0 T. Radiology. 2010; 257:135–143. [PubMed: 20713607]
8. Taouli B, Thakur RK, Mannelli L, et al. Renal lesions: characterization with diffusion-weighted imaging versus contrast-enhanced MR imaging. Radiology. 2009; 251:398–407. [PubMed: 19276322]
9. Karlo CA, Donati OF, Burger IA, et al. MR imaging of renal cortical tumours: qualitative and quantitative chemical shift imaging parameters. Eur Radiol. 2013; 23:1738–1744. [PubMed: 23300041]
10. Nakajima R, Abe K, Kondo T, Tanabe K, Sakai S. Clinical role of early dynamic FDG-PET/CT for the evaluation of renal cell carcinoma. Eur Radiol. 2016; 26:1852–1862. [PubMed: 26403580]
11. Schneider CA, Rasband WS, Eliceiri KW. NIH Image to ImageJ: 25 years of image analysis. Nat Methods. 2012; 9:671–675. [PubMed: 22930834]
12. Seshan VE, Gönen M, Begg CB. Comparing ROC curves derived from regression models. Stat Med. 2013; 32:1483–1493. [PubMed: 23034816]
13. Demler OV, Pencina MJ, D'Agostino RB. Misuse of DeLong test to compare AUCs for nested models. Stat Med. 2012; 31:2577–2587. [PubMed: 22415937]
14. Pepe MS, Kerr KF, Longton G, Wang Z. Testing for improvement in prediction model performance. Stat Med. 2013; 32:1467–1482. [PubMed: 23296397]
15. Lane BR, Babineau DC, Poggio ED, et al. Factors predicting renal functional outcome after partial nephrectomy. J Urol. 2008; 180:2363–2368. [PubMed: 18930264]
16. Leveridge MJ, Finelli A, Kachura JR, et al. Outcomes of small renal mass needle core biopsy, nondiagnostic percutaneous biopsy, and the role of repeat biopsy. Eur Urol. 2011; 60:578–584. [PubMed: 21704449]
17. Kim JH, Bae JH, Lee KW, Kim ME, Park SJ, Park JY. Predicting the histology of small renal masses using preoperative dynamic contrast-enhanced magnetic resonance imaging. Urology. 2012; 80:872–876. [PubMed: 22854134]
18. Sun MRM, Ngo L, Genega EM, et al. Renal cell carcinoma: dynamic contrast-enhanced MR imaging for differentiation of tumor subtypes—correlation with pathologic findings. Radiology. 2009; 250:793–802. [PubMed: 19244046]
19. Choudhary S, Rajesh A, Mayer N, Mulcahy K, Haroon A. Renal oncocytoma: CT features cannot reliably distinguish oncocytoma from other renal neoplasms. Clin Radiol. 2009; 64:517–522. [PubMed: 19348848]
20. Pierorazio PM, Hyams ES, Tsai S, et al. Multiphasic enhancement patterns of small renal masses (≤4 cm) on preoperative computed tomography: utility for distinguishing subtypes of renal cell carcinoma, angiomyolipoma, and oncocytoma. Urology. 2013; 81:1265–1272. [PubMed: 23601445]
21. Hindman N, Ngo L, Genega EM, et al. Angiomyolipoma with minimal fat: can it be differentiated from clear cell renal cell carcinoma by using standard MR techniques? Radiology. 2012; 265:468–477. [PubMed: 23012463]

Author Manuscript Author Manuscript Author Manuscript Author Manuscript

22. Cornelis F, Tricaud E, Lasserre AS, et al. Routinely performed multiparametric magnetic resonance imaging helps to differentiate common subtypes of renal tumours. Eur Radiol. 2014; 24:1068–1080. [PubMed: 24557052]

23. Reuter VE, Tickoo SK. Differential diagnosis of renal tumours with clear cell histology. Pathology. 2010; 42:374–383. [PubMed: 20438412]

24. Vargas HA, Delaney HG, Delappe EM, et al. Multiphasic contrast-enhanced MRI: single-slice versus volumetric quantification of tumor enhancement for the assessment of renal clear-cell carcinoma Fuhrman grade. J Magn Reson Imaging. 2013; 37:1160–1167. [PubMed: 23152173]

25. Lanzman RS, Robson PM, Sun MR, et al. Arterial spin-labeling MR imaging of renal masses: correlation with histopathologic findings. Radiology. 2012; 265:799–808. [PubMed: 23047841]

Author Manuscript Author Manuscript Author Manuscript Author Manuscript

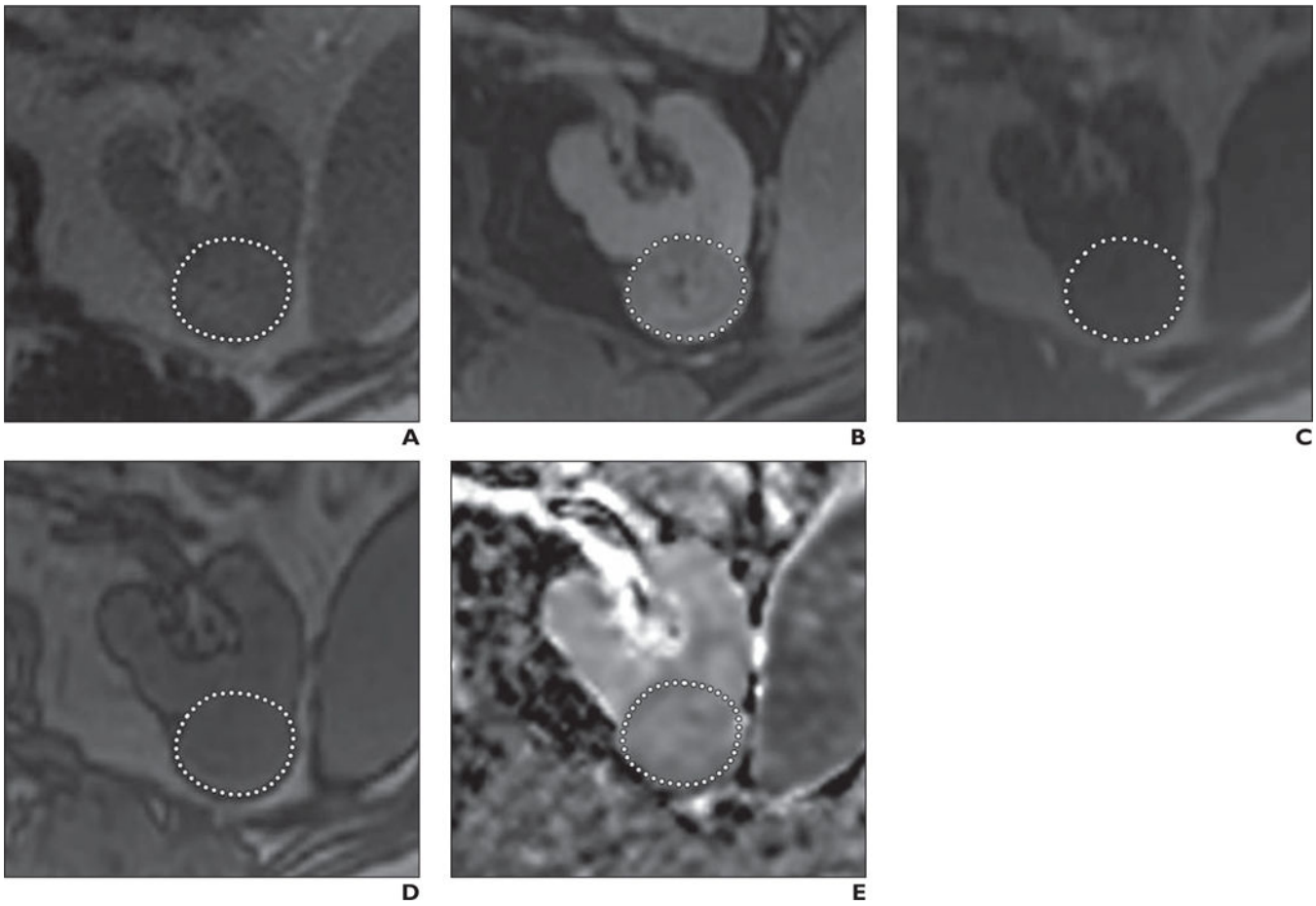

Fig. 1.

74-year-old man with clear cell renal cell carcinoma of left kidney. Dotted line indicates exemplary ROI for this slice (tumors were assessed volumetrically).

A, T2-weighted MR image.

B, T1-weighted contrast-enhanced fat-saturated MR image.

C, T1-weighted in-phase chemical-shift MR image.

D, T1-weighted opposed-phase chemical-shift MR image.

E, Apparent diffusion coefficient map.

Author Manuscript Author Manuscript Author Manuscript Author Manuscript

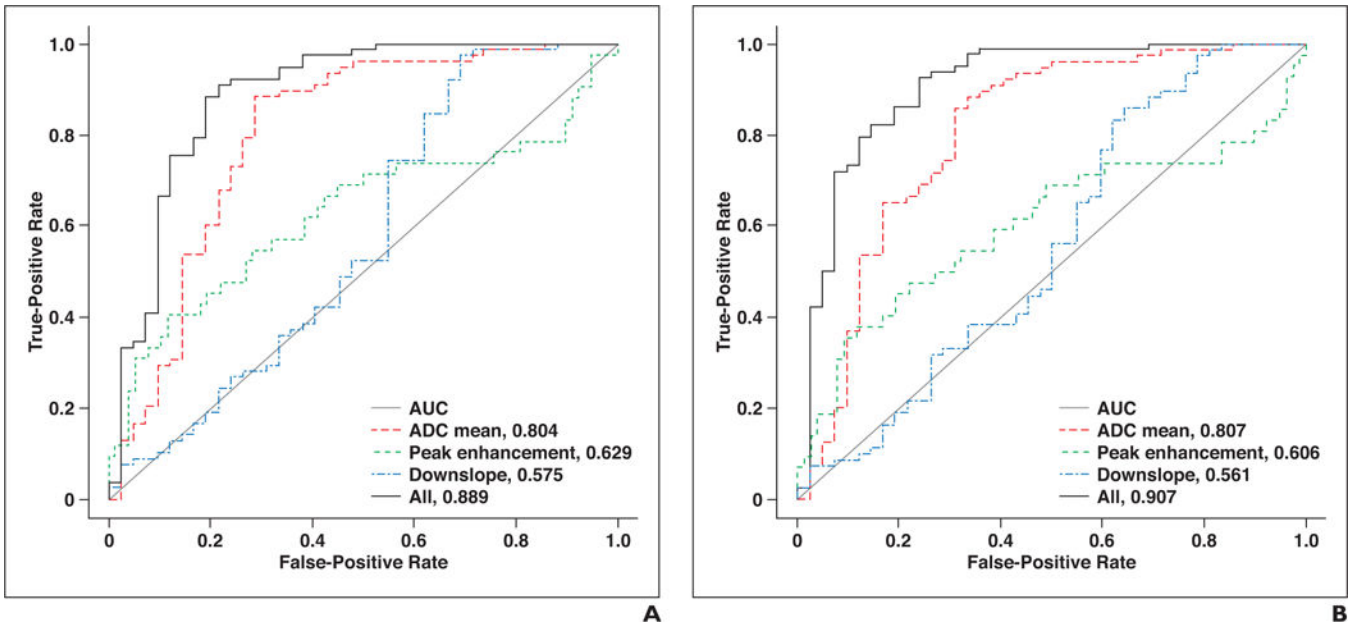

Fig. 2.

;ROC curves for parameters apparent diffusion coefficient (ADC), peak enhancement, downslope, and combination of these three parameters.

A, Reader 1.

B, Reader 2.

Author Manuscript Author Manuscript Author Manuscript Author Manuscript

TABLE 1

MRI Parameters for Two Readers and Their Interreader Agreement Across All Tumors

Parameter	Clear Cell Renal Cell Carcinoma (*n* = 81)		Other Renal Cortical Tumors (*n* = 43)		ICC
	Reader 1	Reader 2	Reader 1	Reader 2	
Apparent diffusion coefficient ($\times 10^{-3}$)	2.3 (1.0–3.1)	2.3 (1.1–3.2)	1.7 (0.8–3.3)	1.7 (0.7–3.3)	0.945
Peak enhancement	174.86 (13.69–617.05)	161.4 (9.58–547.96)	118.06 (2.10–1159.29)	108.19 (1.40–1171.23)	0.959
Upslope	0.51 (0.04–2.64)	0.50 (0.03–4.01)	0.46 (0.03–7.71)	0.47 (0.02–7.76)	0.987
Downslope	−0.04 (−1.20 to 2.66)	0 (−0.92 to 5.10)	−0.06 (-3.62 to 0.84)	0.02 (−3.38 to 1.35)	0.815
AUC	20696.33 (1675.97 to 156,502.42)	19567.23 (1238.61 to 157,317.7)	17727.5 (342.81 to 302,143.93)	17211.37 (229.05 to 304,998.19)	0.994
Chemical-shift index	−6.68 (−46.45 to 20.34)	−6.26 (−52.23 to 35.06)	−1.35 (−64.55 to 44.1)	−0.64 (−61.77 to 59.08)	0.870
Chemical-shift volume drop	37.33 (2.58–96.97)	34.11 (2.58–100)	23.08 (1.80–100)	16.23 (0.86–100)	0.930

Note—Except for intraclass correlation coefficient (ICC), values are median with range in parentheses.

AJR Am J Roentgenol. Author manuscript; available in PMC 2018 March 01.

Author Manuscript

Author Manuscript

Author Manuscript

Author Manuscript

TABLE 2

Results of Univariate and Multivariable Logistic Regression Analyses to Identify Parameters Helpful in Identifying Clear Cell Renal Cell Carcinoma

	Univariate Analysis		Multivariable Analysis	
Parameter	**Odds Ratio**	***p***	**Odds Ratio**	***p***
Reader 1				
ADC	1.30 (1.15–1.47)	<0.001	1.34 (1.13–1.60)	<0.001
Peak enhancement[a]	1.77 (1.09–2.87)	0.021	3.18 (1.86–5.44)	<0.001
Upslope[a]	0.99 (0.63–1.56)	0.964		
Downslope	3.45 (1.37–8.66)	0.009	1.39 (1.18–1.62)	<0.001
AUC[a]	1.08 (0.72–1.62)	0.726		
Chemical-shift index	0.97 (0.92–1.03)	0.362		
Chemical-shift volume drop	1.02 (1.00–1.05)	0.087		
Reader 2				
ADC	1.29 (1.14–1.45)	<0.001	1.42 (1.17–1.73)	<0.001
Peak enhancement[a]	1.63 (1.04–2.54)	0.032	2.99 (1.80–4.98)	<0.001
Upslope[a]	0.95 (0.61–1.49)	0.834		
Downslope	2.27 (1.05–4.92)	0.038	1.39 (1.14–1.70)	0.001
AUC[a]	1.04 (0.70–1.54)	0.854		
Chemical-shift index	0.98 (0.94–1.02)	0.295		
Chemical-shift volume drop	1.02 (1.00–1.05)	0.084		
Pathologic tumor size	1.04 (0.94–1.16)	0.441		

Note—Values in parentheses are 95% CI. The odds ratio expresses the odds of patients having clear cell renal cell carcinoma relative to patients with the parameter value 1 unit lower. For apparent diffusion coefficient (ADC), the odds ratio was estimated for every increment of 0.0001, and for downslope for every increment of 10.

[a]Parameter transformed into logarithmic form.

Author Manuscript

Author Manuscript

Author Manuscript

Author Manuscript

TABLE 3

Results of ROC Analysis and Measures of Accuracy in Identifying Clear Cell Renal Cell Carcinoma by Use of Multiparametric MRI With a Combination Cutoff of Apparent Diffusion Coefficient (ADC), Peak Enhancement, and Downslope

Parameter	Sensitivity	Specificity	AUC
Reader 1			
ADC	0.873 (0.780–0.931)	0.698 (0.545–0.816)	0.804
Peak enhancement	0.912 (0.827–0.958)	0.310 (0.186–0.468)	0.629
Downslope	0.962 (0.890–0.988)	0.286 (0.155–0.466)	0.575
3 Parameters combined			0.889
Maximized Youden index	0.897 (0.808–0.948)	0.762 (0.608–0.869)	
Maximized sensitivity	0.987 (0.915–0.998)	0.429 (0.291–0.578)	
Reader 2			
ADC	0.709 (0.599–0.799)	0.674 (0.522–0.797)	0.807
Peak enhancement	0.900 (0.812–0.949)	0.357 (0.224–0.517)	0.606
Downslope	0.800 (0.692–0.877)	0.310 (0.175–0.487)	0.561
3 Parameters combined			0.907
Maximized Youden index	0.897 (0.808–0.948)	0.738 (0.593–0.845)	
Maximized sensitivity	0.987 (0.931–1.000)	0.262 (0.155–0.407)	

Note—Values in parentheses are 95% CI. Cutoff point for combined approach: [−11.011 + 3221 × ADC + 1.111 × log(peak enhancement) + 3.220 × downslope] ≥ 0.245. Cutoff point for approach with best sensitivity: [−11.011 + 3221 × ADC + 1.111 × log(peak enhancement) + 3.220 × downslope] ≥ −2.214.